

## Neutrino masses and mixing driven by Randomness

---

**Aadarsh Singh<sup>a</sup> and Sudhir K. Vempati<sup>a,\*</sup>**

*<sup>a</sup>Centre for High Energy Physics, Indian Institute of Science,  
CV Raman Avenue, Bengaluru, Karnataka, 560012, India*

*E-mail: [aadarshsingh@iisc.ac.in](mailto:aadarshsingh@iisc.ac.in), [vempati@iisc.ac.in](mailto:vempati@iisc.ac.in)*

Strong localisation via the so-called Anderson localisation is possible over different kinds of mass chains in theory space. This localisation can be used to generate tiny neutrino masses and mixing angles. We show that in the limit of strong disorder, these models predict hierarchial neutrino masses and anarchical mixing angles. This is true for all geometries which can be local, non-local or mixed. On the other hand, if one considers weak disorder scenarios, localisation in mixing angles can also be obtained for certain models centered around the present experimental values. These models can serve new models to explain neutrino mixing patterns.

*HQL 2023  
28/11 - 2/12/2023  
TIFR Mumbai*

---

\*Speaker

## 1. Introduction

It is now well established that the data from solar and atmospheric neutrino oscillations can be explained by tiny neutrino masses within the range of  $(10^{-3} - 1)$  eV depending on the hierarchies of the masses one chooses. In comparison with other fermion masses, the neutrino mass range is at least six orders of magnitude smaller compared to the lightest, i.e, the electron mass. Neutrino oscillation data also fixes the mixing between in the leptonic sector to be large compared to the small CKM mixing in the quark sector.

Non-zero neutrino masses require the Standard Model to be extended either in terms of new particles and/or some additional symmetries. The mechanism to generate non-zero neutrino masses also depends on whether neutrinos are Majorana or Dirac. The lowest dimension effective theory beyond the Standard Model has Majorana neutrino mass operators at dimensional five level[1]. Concrete UV Models have typically been the famous seesaw models which have been discovered several decades ago[2],[3],[4],[5],[6],[7] (for recent reviews on these models and their implications please see [8],[9]). In these mechanisms, a heavy mass is used to suppress the weak scale to generate a tiny neutrino mass. An alternative approach to generate the suppression is to use the loop factor as in various radiative mechanisms[10],[11],[12]. For a review of various such models, please see [13]. In addition to these mechanisms, there are several other viable models in literature [14],[15],[16].

In the present work, we will focus on a novel mechanism recently suggested in [17]. This mechanism imports the ideas of Anderson localisation[18] of condensed matter physics to four dimensions and uses localisation in theory(field) space to generate tiny neutrino masses. It should be noted that this mechanism crucially depends on "disorder" or "randomness" in couplings/masses. While such randomness in masses/couplings is assumed in the present work, there are sources of such randomness in more fundamental theories. For example, in effective theories based on String theories, the randomness can be attributed to the variation of the couplings on the landscape[19]. In field theories, other examples exist where randomness is due to the presence of dark sectors with large symmetries[20].

In the present work we show concrete models of Dirac and Majorana neutrino masses using the Anderson localisation mechanism [21]. We show that these classes of models have some universal features in the strong localisation limit. In this case, neutrino masses tend to be hierarchical with anarchical mixing angles irrespective of the underlying geometry in theory space. In the weak localisation regime, depending on the geometry, we show there exist models where in addition to the masses, the mixing angles can also be "localised" in the theory space. Along the way, we compare our results with clockwork models and their variations. The rest of the paper is organised as follows. In the next section, we show the efficiency of Anderson localisation with respect to other similar models like clockwork, random clockwork etc. In section 3), we present the results for the strong localisation regime, for three geometric models. In section 4) concrete examples in the weak localisation regime are presented where it is shown that mixing angles can be "localised" at their experimental values. We close with an outlook and further work in section 5).

## 2. Efficiency of Randomness: A comparison of Anderson mechanism with clockwork and its variations

Consider the following Lagrangian consisting of  $N$  chiral fermions, where  $L_i(R_i)$  represents left(right) handed fields. The total lagrangian including the kinetic terms is represented by Eq.(1), where  $\mathcal{H}$  represents mass terms that follow the underlying geometry in the theory space.

$$\mathcal{L} = \mathcal{L}_{kin} - \sum_{i,j=1}^N \bar{L}_i \mathcal{H}_{i,j} R_j + h.c. \quad (1)$$

In a general manner, encompassing several models,  $\mathcal{H}$  can be represented as follows, with  $K$  an integer taking values  $\{0, 1\}$ :

$$\mathcal{H}_{i,j} = \epsilon_i \delta_{i,j} - t_i (\delta_{i+1,j} + K \delta_{i,j+1}) \quad (2)$$

In Eq.(2), when  $K = 0$  we recover the well-known Clockwork model[22] with  $\epsilon_i = m$  and  $t_i = qm$ . When  $K = 1$ , we have the two-sided or double clockwork with similar assumptions on  $\epsilon$  and  $t$ [23]<sup>1</sup>. Interesting variations happen when  $\epsilon_i$  and  $t_i$  are made random when  $K = 0$  [24] and  $K = 1$  [17]. The random clockwork model ( $K = 0$ ) is when these parameters are chosen randomly in a range rather than being universal[24]. The particularly interesting case of  $K = 1$  and random  $\epsilon_i$  has been studied in [17] which is also the topic of this work. In this work, it has been shown that when  $\epsilon_i$  are randomly varied in an interval such as  $[2t, 2t + W]$ , where  $W$  is a parameter, the model exhibits Anderson-like localisation of its wave functions. The localisation is so effective that it can lead to exponential hierarchies in the couplings.

The mass matrix for the fermionic fields  $\{L_i, R_i\}$  with  $K = 1$  in Eq.(2), in the basis  $(L_1, L_2, \dots, L_N, R_1, R_2, \dots, R_N)$  is a symmetric<sup>2</sup> anti-diagonal block matrix

$$M_{mass} = \begin{bmatrix} 0 & M^A \\ M^A & 0 \end{bmatrix}$$

where the  $M^A$  elements are given as  $M_{ij}^A = L_i M_{ij}^A \bar{R}_j$  and the matrix has the form

$$M^A = \begin{bmatrix} \epsilon_1 & -t & 0 & \dots & 0 \\ -t & \epsilon_2 & -t & \dots & 0 \\ 0 & -t & \epsilon_3 & \dots & 0 \\ \dots & \dots & \dots & \dots & \dots \\ 0 & \dots & \dots & -t & \epsilon_N \end{bmatrix}$$

Choosing the overscale to be  $\mathcal{O}(1)$  TeV, let us consider that  $\epsilon_i$  are random  $\mathcal{O}(1)$  entries within a range given by  $\epsilon_i \in [-2W, 2W]$  and  $t$  to be universal. To be concrete we choose  $t$  to be 1/4 TeV,  $W$  to be 4 TeV and the number of sites,  $N = 8$ . The resulting eigenvectors are plotted in Fig.(1). In the left panel of the figure, we show the eigenvectors along the sites without introducing randomness in  $\epsilon_i$ . For concreteness, we choose  $\epsilon_i = W$ . In the right panel, we treat  $\epsilon_i$  to be random in the range mentioned above.

<sup>1</sup>This limit is very similar to the deconstruction models.

<sup>2</sup>We will assume all the masses are real in this work.

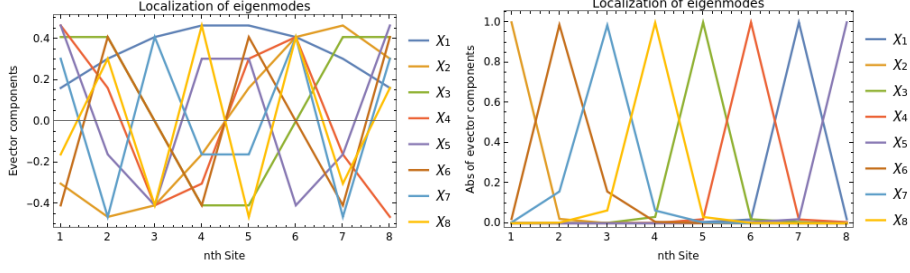


**Figure 1:** - Mass modes  $\chi_i$  of Local lattice with uniform sites  $\epsilon_i = W$  &  $t_i = t$  (left) and random sites  $t_i = t$  &  $\epsilon_i \in [-2W, 2W]$  (right).

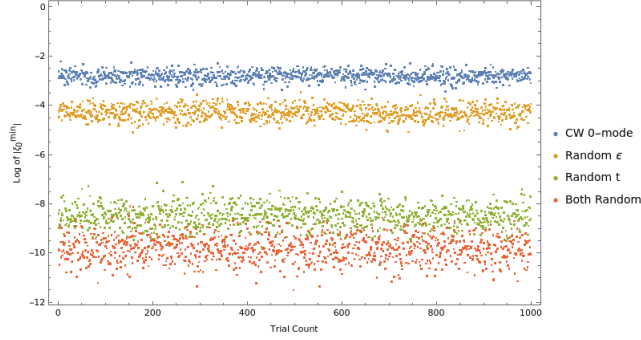


**Figure 2:** Figure shows the median of the Log of Absolute of minimum component 0-mode of CW and lightest mode of disorder models achieved  $\xi_0$  with  $N = 14$  sites for 50 runs with 1000 trials.

As can be seen clearly, the random choice turns the unlocalised wavefunctions in the uniform case into ones that are completely localised at a certain site in the random case. It also demonstrates that all the wavefunctions are localised.

It can further be demonstrated that the Anderson localisation is an efficient method of localisation compared to other similar models like clockwork and its variations, where the zero also typically gets localised. To show this, let us consider a parameter  $\xi_0^{min}$ , defined as:

$$\xi_0^{min} = \min\{\xi_0^i\}, \quad \forall i \in [1, N].$$

It should be noted that  $\xi_0^{min}$  picks the minimum of the zero mode eigenvector for the clockwork models and the lightest mode in the random models. In Fig.(2) we show the values of the  $\xi_0^{min}$  in the random clockwork model as well as various other random models. The number of sites,  $N$  is chosen to be 14. The parameters chosen for various cases are presented in Table (1). As can be seen from the figure, randomness is much stronger when both the  $t$  and  $\epsilon_i$  parameters are chosen to be random.

### 3. Strong Disorder: Neutrino Masses and Mixing

In condensed matter systems, there is a particularly interesting scenario where the disorder is significantly large in the  $\epsilon$  terms. This is called the strong disorder limit and it coincides with the limit

**Table 1:** Parameters considered for Clockwork and both-sided Hamiltonian with  $W = 5$  TeV and  $t = 1$  TeV.

Scenario	K	$\epsilon_i$ (TeV)	$t_i$ (TeV)
Clockwork	0	$[2t, 2t+2W]$	$[-t, t]$
Random Site	1	$[2t, 2t+2W]$	$\frac{t}{2}$
Random Coupling	1	W	$[-t, t]$
Random Site & Coupling	1	$[2t, 2t+2W]$	$[-t, t]$

$\epsilon_i(W) \gg t$  in the Hamiltonian  $\mathcal{H}$  in Eq.(2). In this work, we show that in this limit, there are some universal features regarding neutrino masses and mixing angles independent of the underlying geometry of the theory space defining the mass matrix of Eq.(1). We consider three particular geometries which are sort of extreme cases in terms of the "locality" of the "hopping"/"interaction" terms. The three cases we consider are (i) Completely local (ii) Completely non-local (iii) partially non-local. The case of completely local is the one where the hopping terms or  $t$  terms are restricted to be only nearest neighbour ones as in Ref.[25]. The case of completely non-local is considered in Ref.[26] where in addition to nearest neighbour mass terms, mass terms with all other possible sites are also considered with reducing weight depending on the distance from the sites. Finally, the semi-local has so far not been considered in the literature as far as we know. Of all possible choices, we consider a particularly interesting choice of the Petersen graph as a partially non-local where in addition to the local mass terms, only a particular set of non-local terms are allowed as per the geometry of the graph in theory space. In the following, we will discuss the results from the three cases assuming three neutrino flavors. More details can be found in [21].

All three cases share the same Hamiltonian as in Eq.(1) as before but now extended to three flavors, as we will need at least three Anderson localisations at work.

$$\mathcal{L}_{NP} = L_{kin} - \sum_{i,j=1}^N \overline{L}_i^{\alpha} \mathcal{H}_{i,j}^{\alpha,\beta} R_j^{\beta} + h.c. \quad (3)$$

The chiral fields of the above lagrangian with now interact with the Standard Model neutrino fields to generate tiny neutrino masses determined by the matrix:

$$\mathcal{L}_{Int.} = Y^{a,\alpha} \overline{\nu}_L^a H R_1^{\alpha} + Y^{b,\beta} \overline{\nu}_R^b H L_N^{\beta} + h.c. \quad (4)$$

where  $a, b, \alpha$  and  $\beta$  are flavor indices and  $R_1$  and  $L_N$  are the modes in Eq.(3).

We will now present the distributions of neutrino masses and mixing angles for the three geometries mentioned above. 1) Firstly the completely local case is specified only by nearest neighbour "hopping" or interaction terms as given by Eq.(2) with  $K = 1$ .

In the Fig.(3) we show the distributions for neutrino masses and mixing angles. The number of sites,  $N$  is chosen to be 8 and  $\epsilon_i$  are varied between  $[-2W, 2W]$  with  $W = 5$  TeV and  $t_i = t = 0.1$  TeV. It should be noted that the parameters  $Y$  in Eq.(4) can also influence the results. Choosing them to be  $\mathcal{O}(1)$  we notice that there are two possible cases to generate intergenerational mixing (a) site-mixing:  $Y$  are flavor diagonal and  $H_{\alpha,\beta}$  are flavor off-diagonal and (b) Yukawa mixing:  $Y$  are

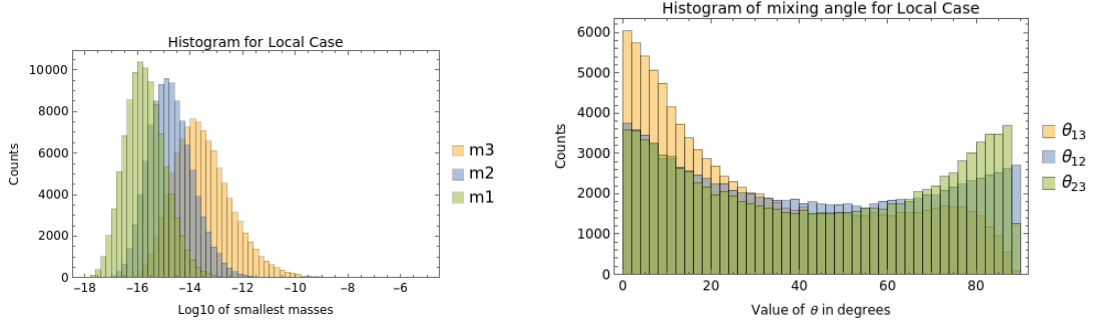


**Figure 3:** Figure shows the mass distribution histogram (left) and mixing angle histogram (right) for 100000 runs produced in local theory space for site mixing with  $W = 5$  TeV,  $t = 0.1$  TeV and  $N = 8$ .

flavor off-diagonal and  $H_{\alpha,\beta}$  are flavor diagonal. In Fig.(3), we present results assuming case (a) site mixing. As can be seen from the figure (left) neutrino masses turn out to be hierarchical and (right) the mixing angles are anarchical. The choice results with Yukawa mixing are quantitatively different but qualitative features remain the same.

### 3.1 Non-Local Hamiltonian

We now move to the case of completely non-local Hamiltonians, by which we mean that the hopping terms are permitted between any two sites not just the nearest neighbouring ones. A particular example of this type was presented for scalars mass matrix in Ref [26],[27], in which the strength of the hopping terms decays with the intersite distance. We will incorporate a similar Hamiltonian to our case however now applied to fermions. It should be noted that this Hamiltonian also exhibits Anderson localisation as the local case. The relevant Fermionic lagrangian is given by

$$\mathcal{L}_{long-range} = L_{Kin} - \sum_{i,j=1}^N \bar{L}_i \epsilon_{i,j} R_j - \sum_{i,j=1}^N \bar{L}_i \frac{t}{b^{|i-j|}} (1 - \delta_{i,j}) R_j + h.c. \quad (5)$$

The total Dirac mass matrix including the long-range Hamiltonian in the basis of fermionic fields  $L_i, R_j$  is given by

$$M_{long-range} = \begin{bmatrix} \epsilon_1 & \frac{t}{b} & \frac{t}{b^2} & \cdots & \frac{t}{b^{N-1}} \\ \frac{t}{b} & \epsilon_2 & \frac{t}{b} & \cdots & \frac{t}{b^{N-2}} \\ \frac{t}{b^2} & \frac{t}{b} & \epsilon_3 & \cdots & \frac{t}{b^{N-3}} \\ \cdots & \cdots & \cdots & \cdots & \cdots \\ \frac{t}{b^{N-1}} & \cdots & \cdots & \frac{t}{b} & \epsilon_N \end{bmatrix},$$

where we have assumed  $t_i = t$  and  $b > 1$  parameterises the decaying factor. For our numerical results, we use similar values for  $N, \epsilon_i$  and  $t$ . We choose  $N = 14$  and  $\epsilon_i \in [-2W, 2W]$  with  $W = 5$  TeV.  $b$  is chosen to be 5 whereas  $t_i = t = 0.1$  TeV. For the case (a) site mixing the results are presented in Fig.(4). As can be seen, the results are very similar to the local case with neutrino masses predominantly hierarchical (left) and the mixing angles completely anarchical.

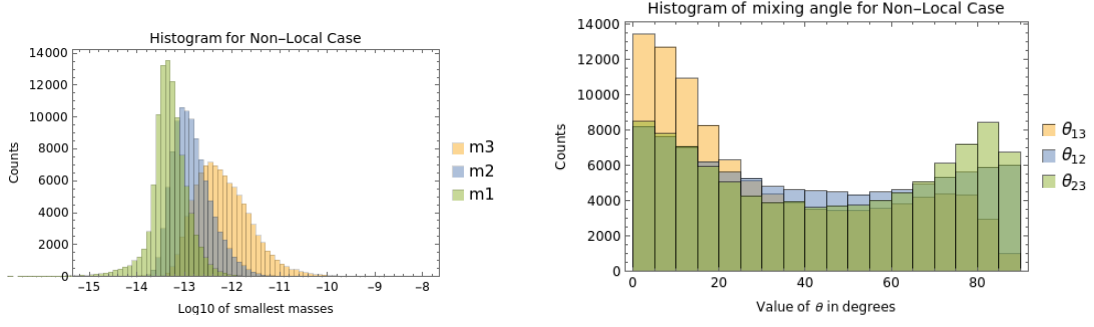


**Figure 4:** Figure shows the mass distribution histogram (left) and mixing angle histogram (right) for 100000 runs produced in non-local theory space for site mixing with  $W = 5$  TeV,  $t = 0.1$  TeV,  $b = 5$  and  $N = 14$ .

### 3.2 Petersen Hamiltonian

The above two cases can be considered extreme cases in terms of locality/non-locality of the hopping terms. It would be interesting to consider graphs that are somewhere in the middle in terms of connectivity. The Petersen graph has connectivity more than the local graph but less than the non-local graph. The graph is interesting in general graph theory as well as in network theory. Lagrangians with such connections in theory space have not been studied before in literature. The Lagrangian for Petersen graph for a general number of sites, assuming  $N$  is even, is given by

$$\begin{aligned}
L_{Petersen} = & L_{Kin} - \sum_{i,j=1}^N \bar{L}_i \epsilon_{i,j} R_j - \sum_{i,j=1}^{N/4} \bar{L}_i \frac{t}{b^{|i-j|}} (\delta_{i,j+N/4} + \delta_{i+N/4,j}) R_j \\
& - \sum_{i,j=1}^{N/2} \bar{L}_i \frac{t}{b^{|i-j|}} (\delta_{i,j+N/2} + \delta_{i+N/2,j}) R_j - \sum_{i,j=N/2+1}^N \bar{L}_i \frac{t}{b^{|i-j|}} (\delta_{i,j+1}) R_j \\
& - \sum_{i,j=N/2+1}^N \bar{L}_i \frac{t}{b^{|i-j|}} (\delta_{i+1,j}) R_j + h.c. \tag{6}
\end{aligned}$$

In the above, we have assumed that the weights of non-local hopping terms decay with respect to the distance between them, similar to the case of completely non-local structure. The corresponding Dirac mass matrix for  $N=8$  fields in the basis of  $L_i, R_j$  takes the following form

$$M_{Petersen} = \begin{bmatrix} \epsilon_1 & 0 & \frac{t}{b^2} & 0 & \frac{t}{b^4} & 0 & 0 & 0 \\ 0 & \epsilon_2 & 0 & \frac{t}{b^2} & 0 & \frac{t}{b^4} & 0 & 0 \\ \frac{t}{b^2} & 0 & \epsilon_3 & 0 & 0 & 0 & \frac{t}{b^4} & 0 \\ 0 & \frac{t}{b^2} & 0 & \epsilon_4 & 0 & 0 & 0 & \frac{t}{b^4} \\ \frac{t}{b^4} & 0 & 0 & 0 & \epsilon_5 & \frac{t}{b} & 0 & \frac{t}{b^3} \\ 0 & \frac{t}{b^4} & 0 & 0 & \frac{t}{b} & \epsilon_6 & \frac{t}{b} & 0 \\ 0 & 0 & \frac{t}{b^4} & 0 & 0 & \frac{t}{b} & \epsilon_7 & \frac{t}{b} \\ 0 & 0 & 0 & \frac{t}{b^4} & \frac{t}{b^3} & 0 & \frac{t}{b} & \epsilon_8 \end{bmatrix}$$

It is evident that the matrix has a different structure compared to the one in Eq.(3.1). Given that

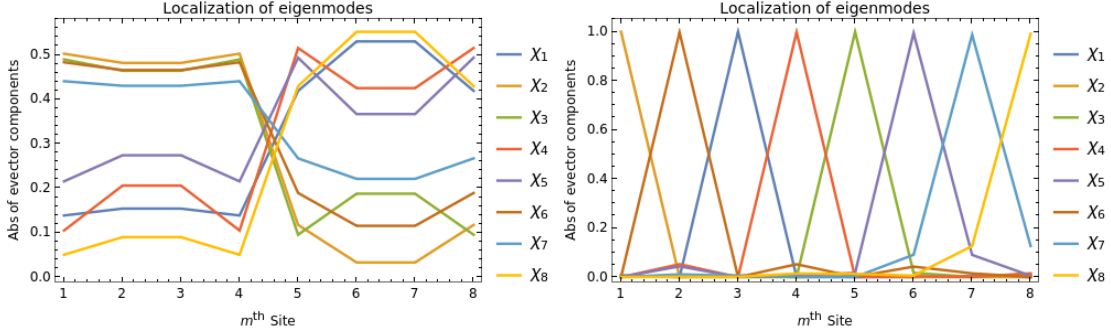


**Figure 5:** Mass modes of Petersen graph with uniform sites  $\epsilon_i = W$  (left) and random sites  $\epsilon_i \in [-2W, 2W]$  (right) for  $N = 8$ ,  $W = 5$  TeV,  $t = 1/4$  TeV and  $b = 2$ .

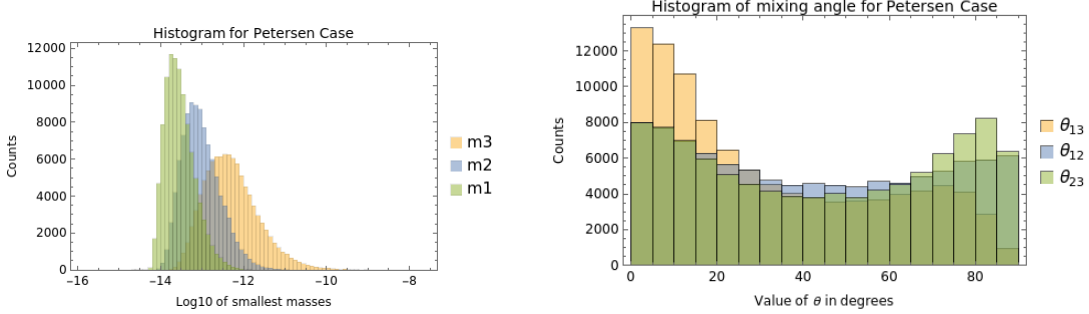


**Figure 6:** Figure shows the mass distribution histogram (left) and mixing angle histogram (right) for 100000 runs produced in non-local theory space for site mixing with  $W = 5$  TeV,  $t = 0.5$  TeV,  $b = 3$  and  $N = 14$ .

the eigenfunctions of this matrix have not been studied in the literature, we found it important to demonstrate the localisation features of this lagrangian. In Fig.5, we showed the localisation features in the wavefunctions and compared to the case where the parameters are uniform instead of random. The numerical values of the parameters are chosen to be  $N = 8$ ,  $W = 5$  TeV,  $b = 2$ , and  $t = 0.25$  TeV. As can be seen from the figure, in the uniform case (all  $\epsilon_i = W$ ), the wave functions have a kink-like form, with half (other half) of them having the maxima (minima) at the first four sites (last four) sites. This is quite interesting and could have potential implications in various areas of physics. In the right graph, we see that localisation is achieved in this case too in the strong disorder limit.

Without much further ado, we now move to present the results from neutrino masses and mixing angles. We consider  $N = 12$  sites with  $\epsilon_i \in [-2W, 2W]$  and  $t_i = t$  with  $W = 5$  TeV,  $b = 5$  and  $t = 0.1$  TeV. As before we present results for the case of site-mixing, *i.e.*, mixing in the  $H_{\alpha,\beta}$ . The Yukawa couplings are considered to be diagonal unit matrix. The results are plotted in Fig.6. The results confirm our assertions that in general in the strong disorder scenario, neutrino masses tend to be hierarchical with anarchical mixing angles.



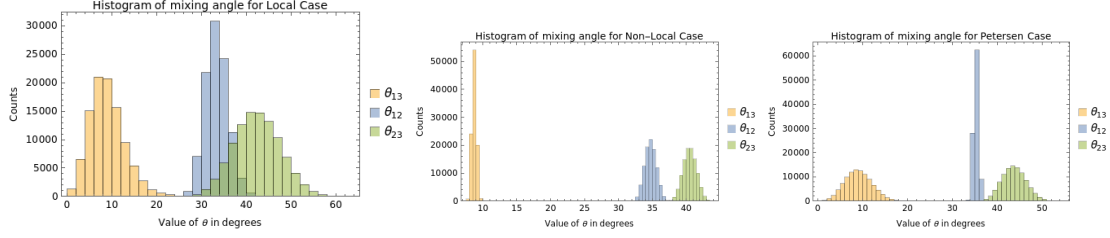


**Figure 7:** Figure shows the distribution of masses produced and histogram of mixing angle for 100000 runs produced for Yukawa mixing with parameters as in table (middle) and site mixing couplings (right) with  $W = 5$  TeV.

**4. Weak Disorder: Neutrino Masses and Mixing**

In the weak disorder limit,  $\epsilon_i \in [W - t, W + t]$  the geometry of the graph plays an important role. We have studied several theory spaces encompassing all three kinds of scenarios for hopping terms (a) completely local (b) completely non-local and (c) mixed as in the Petersen graph. In each case, both site mixing and Yukawa mixing have been considered. The general features of the Weak disorder limit for neutrino masses and mixing angles are:

- localisation is typically not very strong and the resultant hierarchies are significantly lower. This impacts the neutrino mass scales. However, both hierarchical and inverse hierarchical neutrino masses are possible due to "precision pruning" [21].
- Mixing is crucially dependent on whether one chooses "site mixing" or Yukawa mixing. Site Mixing can lead to semi-anarchical or dual localisation mixing angles whereas in Yukawa mixing, it is possible to get stable neutrino mixing angles for a choice of Yukawa couplings which are all  $O(1)$ .
- Explicit examples can be found where neutrino masses and mixing angles are localised and fit in the experimental values.

We now present results for neutrino masses and mixing angles for all three cases (a) local mixing (b) non-local mixing and (c) Petersen graph. In Fig.7, we show the results for the three cases. All the three examples show stable distributions for neutrino mixing angles centred around the experimental values. The explicit values of the Yukawa couplings chosen for the three cases are listed below in Table 2.

**5. Outlook**

We presented a new class of models for neutrino masses and mixing based on "Anderson" like localization in theory space. We have considered two limiting cases of the parameters which are the strong disorder and weak disorder limits. The qualitative features in both the limits are quite distinctive. In the strong disorder case, irrespective of the underlying geometry some universal features can be drawn for neutrino masses and mixing angles: hierarchical masses and anarchical mixing angles. We considered three different geometries: a) completely local b) completely non-local and finally c) mixed, where we considered Petersen Graph. In all these cases, in strong disorder

POS(HQIL2023)025

**Table 2:** Parameters considered for the above scenario unless mentioned, where  $W = 5$  TeV,  $b = 7$  and  $t = 0.2$  TeV

Scenario	N	$\epsilon_i$	$t_i$	Yukawa Couplings ( $Y_{\alpha,\beta}$ )		
Local	9	[W-t, W+t]	t	1	0.5	0.4
				0.5	1	0.3
				0.5	0.9	1
Non-local	14	[W-t, W+t]	t	1	0.4	0.3
				0.2	1	0.7
				0.8	0.6	1
Petersen	12	[W-t, W+t]	t	1	0.3	0.2
				0.3	1	0.1
				0.4	0.6	1

limit, the neutrino masses are hierarchical and mixing angles are anarchical. The weak disorder limit is far more complex and geometry-dependent. However, it is possible to have geometries where the mixing angles are "localised" around the experimental values. More details can be found in [21].

## 6. Acknowledgements

AS thanks CSIR, Govt. of India for SRF fellowship No. 09/0079(15487)/2022-EMR-I. SKV is supported by SERB, Govt. of India Grants numbered, CRG/2021/007170 and MTR/2022/000255.

## References

- [1] Steven Weinberg. Baryon-and lepton-nonconserving processes. *Physical Review Letters*, 43(21):1566, 1979.
- [2] Peter Minkowski.  $\mu \rightarrow e\gamma$  at a rate of one out of 109 muon decays? *Physics Letters B*, 67(4):421–428, 1977.
- [3] Tsutomu Yanagida. Horizontal gauge symmetry and masses of neutrinos. *Conf. Proc. C*, 7902131:95–99, 1979.
- [4] M Gell-Mann, P Ramond, and R Slansky. Supergravity ed p van nieuwenhuizen and dz freedman. *Amsterdam: North-Holland* p, 315:79–18, 1979.
- [5] SL Glashow. The future of elementary particle physics. In *Quarks and Leptons: Cargèse 1979*, pages 687–713. Springer, 1980.
- [6] Rabindra N Mohapatra and Goran Senjanović. Neutrino mass and spontaneous parity non-conservation. *Physical Review Letters*, 44(14):912, 1980.

- [7] J. Schechter and José W. F. Valle. Neutrino masses in  $su(2)\otimes u(1)$  theories. *Physical Review D*, 22(9):2227, 1980.
- [8] André De Gouvêa. Neutrino mass models. *Annual Review of Nuclear and Particle Science*, 66:197–217, 2016.
- [9] Sacha Davidson, Enrico Nardi, and Yosef Nir. Leptogenesis. *Phys. Rept.*, 466:105–177, 2008.
- [10] Ernest Ma. Verifiable radiative seesaw mechanism of neutrino mass and dark matter. *Physical Review D*, 73(7):077301, 2006.
- [11] A Zee. Quantum numbers of majorana neutrino masses. *Nuclear Physics B*, 264:99–110, 1986.
- [12] KS Babu. Model of “calculable” majorana neutrino masses. *Physics Letters B*, 203(1-2):132–136, 1988.
- [13] KS Babu and Chung Ngoc Leung. Classification of effective neutrino mass operators. *Nuclear Physics B*, 619(1-3):667–689, 2001.
- [14] Colin D Froggatt and Holger Bech Nielsen. Hierarchy of quark masses, cabibbo angles and cp violation. *Nuclear Physics B*, 147(3-4):277–298, 1979.
- [15] S. F. King. Neutrino mass models. *Rept. Prog. Phys.*, 67:107–158, 2004.
- [16] Steven Weinberg. The problem of mass. *Transactions of the New York Academy of Sciences*, 38(1 Series II):185–201, 1977.
- [17] Nathaniel Craig and Dave Sutherland. Exponential hierarchies from anderson localization in theory space. *Physical Review Letters*, 120(22):221802, 2018.
- [18] P. W. Anderson. Absence of diffusion in certain random lattices. *Phys. Rev.*, 109:1492–1505, Mar 1958.
- [19] Vijay Balasubramanian, Jan de Boer, and Asad Naqvi. Statistical Predictions From Anarchic Field Theory Landscapes. *Phys. Lett. B*, 682:476–483, 2010.
- [20] Keith R. Dienes, Jacob Fennick, Jason Kumar, and Brooks Thomas. Dynamical Dark Matter from Thermal Freeze-Out. *Phys. Rev. D*, 97(6):063522, 2018.
- [21] Aadarsh Singh and Sudhir Vempati. Disordered neutrino flavours. *Coming Soon, To be Published*.
- [22] Gian F Giudice and Matthew McCullough. A clockwork theory. *Journal of High Energy Physics*, 2017(2):1–39, 2017.
- [23] Aadarsh Singh. Neutrino mass from precision-prune cancellation models and clockwork variants. *Coming Soon Yet to be Published*.

- [24] Fernando Abreu de Souza and Gero von Gersdorff. A random clockwork of flavor. *Journal of High Energy Physics*, 2020(2):1–35, 2020.
- [25] N. Craig and D. Sutherland. Exponential hierarchies from anderson localization in theory space. *Physical Review Letters*, 120(22):221802, 2018.
- [26] A. Tropper and J. J. Fan. Randomness-assisted exponential hierarchies. *Physical Review D*, 103(1):015001, 2021.
- [27] Pavel A Nosov, Ivan M Khaymovich, and VE Kravtsov. Correlation-induced localization. *Physical Review B*, 99(10):104203, 2019.